ORIGINAL ARTICLE

MICB Genomic Variant Is Associated with NKG2D-mediated Acute Lung Injury and Death

Oscar A. Aguilar[1,2], Anita E. Qualls[1], Maria D. R. Gonzalez-Hinojosa[1,2], Sarah Obeidalla[6], V. Eric Kerchberger[6], Tasha Tsao[3], Jonathan P. Singer[3], Mark R. Looney[3], Wilfred Raymond[4], Steven R. Hays[3], Jeffrey A. Golden[3], Jasleen Kukreja[5], Ciara M. Shaver[6], Lorraine B. Ware[6,7], Jason Christie[8,9], Joshua M. Diamond[8], Lewis L. Lanier[1,2], John R. Greenland[3,10], Daniel R. Calabrese,[3,10] and the LTOG Investigators

[1]Department Microbiology and Immunology, [2]Parker Institute for Cancer Immunotherapy, [3]Department Medicine, [4]Cardiovascular Research Institute, and [5]Department of Surgery, University of California San Francisco, San Francisco, California; [6]Department Medicine and [7]Department of Pathology, Microbiology, and Immunology, Vanderbilt University Medical Center, Nashville, Tennessee; [8]Department Medicine and [9]Department of Biostatistics, Epidemiology, and Informatics, University of Pennsylvania, Philadelphia, Pennsylvania; and [10]San Francisco Veterans Affairs Medical Center, San Francisco, California

ORCID IDs: 0000-0002-0342-1965 (V.E.K.); 0000-0003-0224-7472 (J.P.S.); 0000-0002-9429-4702 (L.B.W.); 0000-0002-3695-4637 (J.M.D.); 0000-0003-1422-8367 (J.R.G.); 0000-0002-0596-3434 (D.R.C.).

Abstract

Rationale: Acute lung injury (ALI) carries a high risk of mortality but has no established pharmacologic therapy. We previously found that experimental ALI occurs through natural killer (NK) cell NKG2D receptor activation and that the cognate human ligand, MICB, was associated with ALI after transplantation.

Objectives: To investigate the association of a common missense variant, $MICB^{G406A}$, with ALI.

Methods: We assessed $MICB^{G406A}$ genotypes within two multicenter observational study cohorts at risk for ALI: primary graft dysfunction ($N = 619$) and acute respiratory distress syndrome ($N = 1{,}376$). Variant protein functional effects were determined in cultured and *ex vivo* human samples.

Measurements and Main Results: Recipients of $MICB^{G406A}$-homozygous allografts had an 11.1% absolute risk reduction (95% confidence interval [CI], 3.2–19.4%) for severe primary graft dysfunction after lung transplantation and reduced risk for allograft failure (hazard ratio, 0.36; 95% CI, 0.13–0.98). In participants with sepsis, we observed 39% reduced odds of moderately or severely impaired oxygenation among $MICB^{G406A}$-homozygous individuals (95% CI, 0.43–0.86). BAL NK cells were less frequent and less mature in participants with $MICB^{G406A}$. Expression of missense variant protein $MICB^{D136N}$ in cultured cells resulted in reduced surface MICB and reduced NKG2D ligation relative to wild-type MICB. Coculture of variant $MICB^{D136N}$ cells with NK cells resulted in less NKG2D activation and less susceptibility to NK cell killing relative to the wild-type cells.

Conclusions: These data support a role for MICB signaling through the NKG2D receptor in mediating ALI, suggesting a novel therapeutic approach.

Keywords: acute respiratory distress syndrome; primary graft dysfunction; acute lung injury; NK cells

(Received in original form March 14, 2023; accepted in final form October 17, 2023)

A complete list of Lung Transplant Outcomes Group Investigators may be found in the online supplement (Table E1).

Supported by Cystic Fibrosis Foundation grant CALABR19Q0 and Biomedical Laboratory Research and Development, VA Office of Research and Development grant 1IK2BX005301 (D.R.C.); Burroughs Wellcome Fund, Cancer Research Institute Fellow (O.A.A.); the Parker Institute for Cancer Immunotherapy and NIH grant AI068129 (O.A.A., M.D.R.G.-H., and L.L.L.); NIH grant K01HL157755 and the American Thoracic Society research program (V.E.K.); NIH grant K08HL136888 (C.M.S.); NIH grants U01HL163303, R01HL158906, and R01HL164937 (L.B.W.); NIH grants R01HL130324 and R35HL161241 (M.R.L.); Cystic Fibrosis Foundation, VA Office of Research and Development grant CX002011 and NIH NHLBI grant HL151552 (J.R.G.); and NIH grants U01HL145435, R01 HL134851, and R01 HL 130324 (J.P.S.). Donor genotyping at the University of California San Francisco was funded by the Nina Ireland Program for Lung Health. Lung Transplant Outcomes Group data were supported by NIH grants U01HL145435, R01HL087115, and R01HL081619. Validating Acute Lung Injury biomarkers for Diagnosis genotyping services were provided by Genentech Inc.

Author Contributions: Conceptualization: D.R.C., J.R.G., O.A.A., and L.L.L.; methodology: D.R.C. and O.A.A.; investigation: O.A.A., M.D.R.G.-H., A.E.Q., T.T., W.R., D.R.C., T.T., and M.R.L.; data analysis: D.R.C., O.A.A., S.O., C.M.S., and V.E.K.; visualization: O.A.A., D.R.C., and S.O.; funding acquisition: D.R.C., L.L.L., J.R.G., O.A.A., L.B.W., J.C., and M.R.L.; writing – original draft: O.A.A. and D.R.C.; writing – review and editing: O.A.A., D.R.C., L.L.L., J.R.G., J.P.S., J.M.D., V.E.K., S.R.H., J.A.G., J.C., and L.B.W.

Data and materials availability: All data, materials, and code are available upon request to the corresponding author. Cell lines are subject to materials transfer agreements.

Am J Respir Crit Care Med Vol 209, Iss 1, pp 70–82, Jan 1, 2024

Originally Published in Press as DOI: 10.1164/rccm.202303-0472OC on October 25, 2023
Internet address: www.atsjournals.org

At a Glance Commentary

Scientific Knowledge on the Subject: Acute lung injury (ALI) is mediated through innate immune activation. We previously identified that natural killer cells can recognize stress markers on airway cells after experimental ALI, but the role of this mechanism in human ALI has not been well defined.

What This Study Adds to the Field: This study identifies a common genetic polymorphism in a cellular stress ligand to probe the biology of innate immune activation during human ALI. These findings are critical, as they identify a novel target for two major lung diseases, acute respiratory distress syndrome and primary graft dysfunction, that currently have no known medical therapies.

Acute lung injury (ALI) results from a variety of precipitating factors, including viral and bacterial pneumonia, major surgery, and sepsis (1). Severe ALI manifests as acute respiratory distress syndrome (ARDS), marked by impaired oxygenation and pulmonary edema that is fatal in >40% of patients (2). Primary graft dysfunction (PGD), the form of ALI that occurs after one-third of lung transplant procedures, shares pathophysiology with ARDS and accounts for 50% of the mortality in the first postoperative year (3–6). There are no known pharmacologic therapies for either syndrome (7, 8).

ALI results from lung endothelial and epithelial injury, release of inflammatory mediators, and the recruitment of innate immune cells (9). We recently described a novel role of natural killer (NK) cells in mediating ALI (10). NK cells are innate lymphocytes that use a myriad of somatically encoded cell surface receptors to surveil for missing self, pathogenic, or "stressed" cells (11, 12). The stimulatory NKG2D (*KLRK1*) receptor is expressed on NK cells and some T cells (13) and engages an array of stress-induced ligands encoded by the *MICA*, *MICB*, and the *RAET1* or *ULBP* family of genes (14, 15). These ligands share homology to major histocompatibility complex class I molecules, do not bind peptides, and are highly polymorphic (15, 16).

We and others previously reported that NKG2D drives NK-mediated acute injury of the lung and kidney in animal models (10, 17–19). We have also shown that MICB expression is increased in severe human PGD and associated with lung allograft morbidity and neutrophilic inflammation (20). A candidate SNP in MICB, $MICB^{G406A}$, was examined within our cohorts. This prevalent missense mutation results in substitution of asparagine for aspartate and has previously been linked with herpes simplex virus and schizophrenia (21). Therefore, we hypothesized that $MICB^{G406A}$ would be associated with differential risk for ALI.

Methods

Additional detail on all aspects of materials and methods for this study is provided in the online supplement.

Study Populations

All study participants provided informed consent. Genotyping was performed as previously described (22, 23). BAL participants were included if they had at least one previously analyzed sample (24, 25).

Genotype Selection and Nomenclature

We selected genotypes based on the following criteria among *MICB* SNPs: having a minor allele frequency >20%, having a published phenotype, and by resulting in a missense amino acid change (*see* Table E2 in the online supplement) (26). We also performed a secondary analysis of eight additional *MICB* SNPs. The *MICB* rs1051788 (NC_000006.11:g.31474000G>A) polymorphism minor allele A was abbreviated as $MICB^{G406A}$, and the major allele G was abbreviated as $MICB^{WT}$ (26). Molecular MICB studies reference the variant protein with asparagine at position 136 (Asn136) as $MICB^{D136N}$ and the wild-type (WT) protein with an aspartate at position 136 (Asp136) as $MICB^{WT}$.

Clinical Outcomes

PGD was scored by two independent experts using international criteria (27, 28). Severe PGD was defined as grade 3 on postoperative day 2 or 3 (28). Allograft failure was defined as retransplantation or death (22). Among Validating Acute Lung Injury biomarkers for Diagnosis (VALID) cohort participants, oxygenation impairment was graded based on worst Pa_{O_2} to $F_{I_{O_2}}$ (P:F) ratio during the first 4 days in the ICU according to the Berlin definitions of ARDS (29).

Cell Lines, Cloning, Transfections, and Transductions

$MICB^{G406A}$ was generated through site-directed mutagenesis (Table E3). The $MICB^{WT}$ and $MICB^{G406A}$ coding sequences were inserted into EGFP (enhanced green fluorescent protein)-containing mammalian expression vectors (30) and transfected into Ba/F3 cells (31) and HEK293T cells (ATCC, #ACS-4500). Transductants were purified by EGFP expression. NKG2D reporter cells were generated by transducing an $hNKG2D^{ECD}$ fused to the cytoplasmic CD3ζ vector into BWZ.36 (BWZ) cells (32), as described (33). Reporter assays were conducted as described (34). NK-92 cells (ATCC, #CRL-2407) were used for functional assays. Primary human airway cell and NK cell coculture experiments were conducted as previously described (35).

Flow Cytometry and Bioinformatics

BAL was prospectively collected and immunophenotyped (Figure E1) from lung transplant recipients as previously described (24). MICB was identified via anti-MICB staining or via coculture with His-tagged soluble-NKG2D protein and secondary antibody staining by flow cytometry. Data were analyzed using FlowJo (FlowJo, LLC). MICB and NKG2D molecular sequences were obtained from the National Center for Biotechnology Information and analyzed with MegAlign Pro (DNASTAR Lasergene 17) and PyMOL (Schrödinger) (36).

Statistical Analysis

Data were analyzed using R (version 4.1.1, R Foundation for Statistical Computing) and

Correspondence and requests for reprints should be addressed to Daniel R. Calabrese, M.D., 4150 Clement Street, Box 0111D, San Francisco, CA 94121. E-mail: daniel.calabrese@ucsf.edu.

This article has a related editorial.

This article has an online supplement, which is accessible from this issue's table of contents at www.atsjournals.org.

Prism (version 9, GraphPad). Participant characteristics were compared using two-tailed Student's *t*, Mann-Whitney *U*, or χ^2 tests, as appropriate. Cox proportional hazards models were used to determine survival hazard ratios (HRs), and data were visualized with Kaplan-Meier plots. We used multivariable or cumulative linked regression to assess associations between *MICB* genotype and nominal or ordinal clinical outcomes, respectively. All models included baseline covariates with generalized estimating equation corrections for repeat measures (37). Individual figure legends specify biologic and technical replicates, sample size, and statistical testing.

Results

Donor *MICB*^{G406A} Is Associated with Reduced Risk of PGD

Severe PGD occurred within 25.8% of the participants in the LTOG (Lung Transplant Outcomes Group) cohort, a multicenter, prospective, observational study of risk factors for PGD. Table 1 details characteristics for recipients ($N = 619$). Recipients with PGD were more often female, had higher body mass index, more often received allografts from donors with smoking history, and had higher mean pulmonary artery pressure (mPAP) than participants without PGD (5). The LTOG cohort is similar in racial/ancestral background to the U.S. average lung transplant recipient, and we found no differences in PGD by ancestry (38).

The *MICB* SNP rs1051788 is on chromosome 6 and has a minor allele frequency of 43% in this cohort (Figure 1). This is higher than the global median (Figure E2), although we found no differences in *MICB*^{G406A} by donor ancestry (Table E4). Based on our inclusion criteria and secondary analysis (Table E2), we hypothesized that donor *MICB*^{G406A} would confer better outcomes relative to donor *MICB*^{WT}. Recipients of *MICB*^{G406A}-homozygous allografts had a 44% reduction in PGD grade on Day 2 or 3 (Figure 2A; odds ratio [OR], 0.56; 95% confidence interval [CI], 0.36–0.90; $P = 0.02$) and reduced odds of severe PGD compared with recipients of *MICB*^{WT} allografts (Figure 2B; OR, 0.90; 95% CI, 0.81–0.99; $P = 0.04$). Donor *MICB*^{G406A} conferred an 11.1% absolute risk reduction for severe PGD (95% Cl, 3.2–19.4%). This effect persisted in a sensitivity analysis adjusted for age, donor smoking, mPAP, transplant indication, and recipient sex (OR, 0.53; 95% CI, 0.32–0.87; $P = 0.01$). Notably, recipient *MICB*^{G406A} was not associated with PGD (OR, 0.93; 95% CI, 0.58–1.49; $P = 0.75$). Together, these findings establish donor *MICB* as a potentially powerful determinant of ALI after lung transplant.

Table 1. Lung Transplant Outcomes Group Participant Baseline Characteristics

	No PGD ($n = 493$)	PGD ($n = 126$)	*P* Value
Sex, male	222 (45)	43 (34.1)	0.04
Age, yr	53.5 ± 13.1	55.5 ± 10.8	0.08
Diagnosis			<0.001
ILD	202 (41)	84 (66.7)	
COPD	183 (37.1)	25 (19.8)	
CF	82 (16.6)	8 (6.3)	
pHTN	26 (5.3)	9 (7.1)	
Race			0.8
White	406 (82.4)	100 (79.4)	
African American	51 (10.3)	17 (13.5)	
Asian	14 (2.8)	4 (3.2)	
Other	22 (4.5)	5 (4)	
Transplant type			0.7
Single	137 (27.8)	32 (25.4)	
Bilateral	349 (70.8)	93 (73.8)	
Heart–lung	7 (1.4)	1 (0.8)	
BMI	24.8 ± 4.8	26.7 ± 4.5	<0.001
Donor smoking	170 (34.5)	65 (51.6)	<0.001
mPAP	28.5 ± 11.7	32.4 ± 16.4	<0.001
CMV serostatus			0.7
D−/R−	199 (40.4)	51 (40.5)	
D−/R+	78 (15.8)	15 (11.9)	
D+/R+	97 (19.7)	29 (23)	
D+/R−	94 (19.1)	27 (21.4)	
Unknown	25 (5.1)	4 (3.2)	
Recipient MICB SNP			0.9
GG	234 (47.4)	59 (46.8)	
GA	200 (40.6)	50 (39.7)	
AA	59 (12)	17 (13.5)	

Definition of abbreviations: BMI = body mass index; CF = cystic fibrosis; CMV = cytomegalovirus; COPD = chronic obstructive pulmonary disease; ILD = interstitial lung disease; mPAP = mean pulmonary artery pressure; PGD = primary graft dysfunction; pHTN = pulmonary hypertension.
Data are presented as *n* (%) or mean ± SD.

MICB^{G406A} Confers Less Severe Oxygenation Impairment in Sepsis and ARDS

Sepsis, the syndrome of dysregulated host immune response to infection, is associated with ALI (39). We examined the association between *MICB* variants and respiratory failure among 1,376 critically ill adults with sepsis and 733 with ARDS enrolled in the VALID cohort study (23). Participant characteristics are detailed in Tables 2 and E5. Like the PGD findings, *MICB*^{G406A}-homozygous adults with sepsis had less impaired oxygenation (higher P:F) than *MICB*^{WT} adults (Figure 2C; mean P:F difference: 21 mm Hg; 95% CI, 8–34 mm Hg; $P = 0.001$). This represented 39% reduced cumulative odds of moderate or severe oxygenation impairment (Figure 2D; OR, 0.61; 95% CI, 0.43–0.86; $P = 0.006$). We also observed similar differences in oxygenation among patients with ARDS with the *MICB*^{G406A} variant (Figure 2E; mean P:F difference, 17 mm Hg; 95% CI, 4–29 mm Hg; $P = 0.01$). *MICB*^{G406A} participants with ARDS tended to have more ventilator-free days (OR of an unfavorable outcome based on three ordinal categories [40], 0.78; 95% CI, 0.5–1.23; $P = 0.29$) but had similar survival (HR, 0.92; 95% CI, 0.6–1.5; $P = 0.78$) compared with *MICB*^{WT} participants. These data demonstrate, in a separate cohort, that *MICB*^{G406A} is associated with reduced ALI even among patients with native, nontransplanted lungs.

Donor *MICB*^{G406A} Is Associated with Reduced Graft Failure and Death After Lung Transplant

We evaluated how *MICB*^{G406A} impacted other outcomes after transplant. Severe PGD

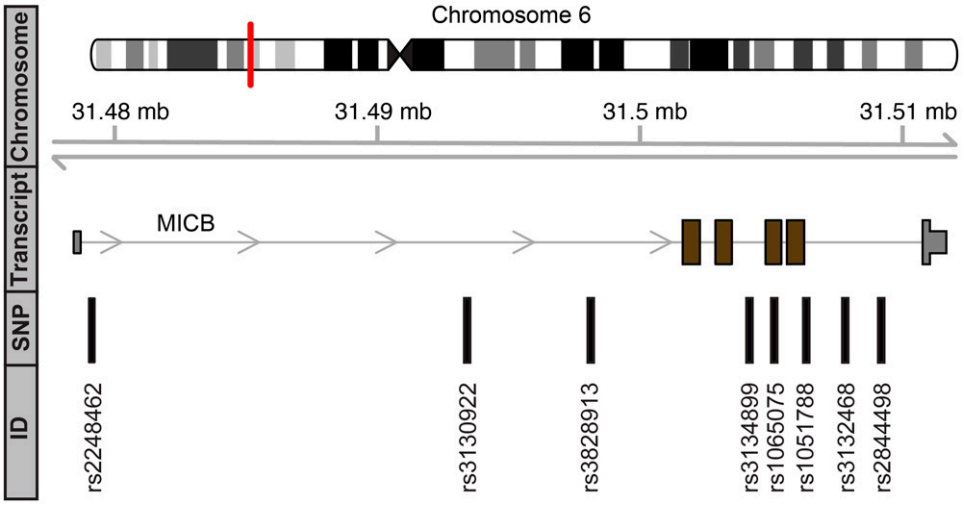

Figure 1. *MICB* SNPs. *MICB* is located on chromosome 6 (red line) and has three major splice variants. We identified eight SNPs across each of the splice variants of potential significance.

was associated with an increased risk of allograft failure or death (Figure 3A; HR, 1.6; 95% CI, 1.2–2.2; $P = 0.004$) (5). $MICB^{G406A}$-homozygous allografts had nearly one-third the risk for allograft failure or death compared with $MICB^{WT}$ allografts (Figure 3B; HR, 0.36; 95% CI, 0.13–0.98; $P = 0.04$) in the first 2 postoperative years. Notably, there was a sixfold increased risk of allograft failure or death among $MICB^{WT}$ allografts with PGD (Figure 3C; 95% CI, 1.8–20.1; $P = 0.003$) compared with $MICB^{G406A}$-homozygous allografts. Together, these findings suggest that *MICB* plays a major role in lung injury and that the donor $MICB^{G406A}$ allele may be associated with reduced short- and long-term allograft dysfunction.

Donor $MICB^{G406A}$ Leads to Reduced BAL MICB Protein and NK Cell Maturation

To determine the impact of $MICB^{G406A}$ on MICB protein, we prospectively collected BAL on Postoperative Day 1 ($n = 77$; Table E6). We found no differences in MICB protein across genotypes in the absence of PGD (Figure 4A). Importantly, we noted reduced MICB protein in recipients with PGD and donor $MICB^{G406A}$ (Figure 4B; $P = 0.03$). We found no difference in MICB protein by donor cytomegalovirus (CMV) serostatus (Figures E3A and E3B), which was an important consideration, as CMV evades immune recognition by altering MICB expression (41). To evaluate NK cells, we prospectively assessed 282 BAL samples from 102 lung transplant recipients obtained during their first 2 postoperative years at University of California San Francisco (Table E6) (20). BAL NK cells ($CD3^-CD56^+$) as a percentage of lymphocytes were reduced in $MICB^{G406A}$-homozygous allografts (AA; median, 5.4%; interquartile range, 2.9–9.8%) relative to $MICB^{WT}$ allografts (GG and GA; Figure 4C; median, 7.5%; interquartile range, 4.2–10.7%; $P = 0.03$). Absolute NK cells were decreased in $MICB^{G406A}$-homozygous allograft BAL (AA; median, 5.5×10^3 cells/ml) relative to $MICB^{WT}$ allograft BAL (GG and GA; Figure 4D; median, 6.6×10^3 cells/ml; $P = 0.04$). Within the first 2 weeks, we also found reduced BAL NK cells among $MICB^{G406A}$-homozygous allografts (Figures E3C and E3D) and that IFNγ and TNFα, two markers of NK cell activity, were also reduced (Figures E3E and E3F).

We hypothesized that NK cell phenotypes would be different across the donor *MICB* genotypes. NK cell maturation was assessed by NKG2A and CD16 (Figure E1D). We found reductions in mature BAL NK cells ($NKG2A^-CD16^+$; Figure 4E; $P = 0.01$) and increases in immature NK cells ($NKG2A^+CD16^-$; Figure 4F; $P = 0.0003$) in recipients of $MICB^{G406A}$-homozygous allografts compared with $MICB^{WT}$ allografts. KIR (Killer cell Immunoglobulin-like Receptor) family expression, an NK cell maturation marker (Figure 4G), was decreased on BAL NK cells in $MICB^{G406A}$-homozygous allografts relative to $MICB^{WT}$ allografts (Figure 4H; $P = 0.005$). Finally, we found no differences in NK cell proliferation across donor *MICB* genotypes (Figures 4I and 4J; $P = 0.9$). These findings suggest that donor $MICB^{G406A}$ confers reduced MICB lung protein during stress and influences NK cells in the allograft to a less mature or activated phenotype.

Structural Analysis of MICA/B Interaction with NKG2D

To determine if the $MICB^{G406A}$ missense amino acid substitution (D136N) affects the interaction of the MICB protein with the NKG2D receptor, we investigated X-ray crystal structures of MICB, MICA, and NKG2D. We found that Asp136 on MICB is conserved across all major histocompatibility complex–related molecules, except for the MICB D136N variant (Figure 5A). Cocrystal structures of MICA:NKG2D have been resolved, but not of MICB:NKG2D (41, 42). Alignment of the β1 and β2 domains of MICA and MICB yielded a root-mean-square deviation of 0.897 Å, which afforded confidence in using MICA complexed with NKG2D as a reference for MICB (Figure 5B). The Asp136 residue does not directly interact with NKG2D (Figure 5C) (41, 42); therefore, we predicted that D136N indirectly impacts the interaction of MICB with NKG2D.

Destabilization of the NKG2D:MICB Interaction by D136N Protein Variant

To determine the functional effects of the D136N amino acid substitution on MICB, we generated mammalian expression vectors encoding both *EGFP* and $MICB^{WT}$ or $MICB^{D136N}$ proteins. We transduced these constructs into the mouse B cell line Ba/F3,

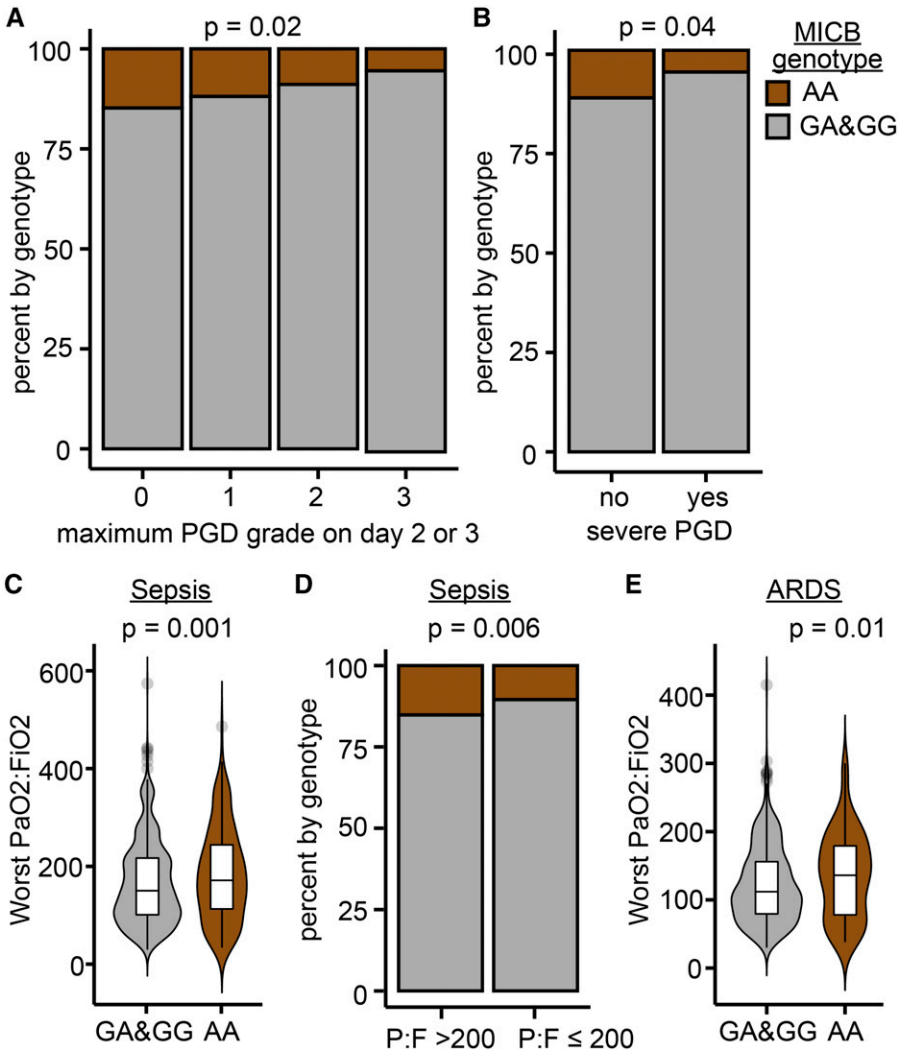

Figure 2. *MICB*^{G406A} genotypes are associated with primary graft dysfunction and acute lung injury. Of 619 participants in the multicenter LTOG (Lung Transplant Outcomes Group) cohort with donor genotyping data, 126 experienced severe primary graft dysfunction (PGD). (*A*) rs1051788 genotype distributions are shown stratified by maximum grade of PGD on Postoperative Day 2 or 3. We found that donor *MICB*^{G406A} genotypes (AA), for whom there is an amino acid change D136N, had decreased odds for increasing severity of PGD grade (odds ratio [OR], 0.56; 95% confidence interval [CI], 0.36–0.90; adjusted $P = 0.02$). (*B*) Severe PGD was defined as grade 3 disease on Postoperative Day 2 or 3. Donor *MICB*^{G406A} genotypes (AA) were associated with reduced odds of severe PGD (OR, 0.90; 95% CI, 0.81–0.99; adjusted $P = 0.04$) compared with allografts with donor *MICB*^{WT} alleles. (*C*) Within the Validating Acute Lung Injury biomarkers for Diagnosis (VALID) cohort, Pa_{O_2} to $F_{I_{O_2}}$ ratios among *MICB*^{G406A} AA genotypes ($n = 165$) and *MICB*^{WT} alleles (GA and GG, $n = 1{,}211$). (*D*) Mild or absent acute lung injury (Pa_{O_2}:$F_{I_{O_2}} > 200$ mm Hg) was compared with moderate or severe acute lung injury (Pa_{O_2}:$F_{I_{O_2}} \leq 200$ mm Hg) among *MICB* genotypes. In the subset of participants with acute respiratory distress syndrome (ARDS) ($n = 733$), Pa_{O_2}:$F_{I_{O_2}}$ is shown stratified by *MICB* AA genotypes ($n = 82$) or GA and GG genotypes. Differences in PGD grade on Days 2 or 3 were assessed with cumulative linked models, and severe PGD and ARDS differences were assessed with logistic regression, both approaches adjusted for participant characteristics.

which does not express NKG2D ligands that might interact with human NKG2D receptors. We sorted cells for equal EGFP^{+} expression across the Ba/F3.MICB^{WT} and Ba/F3.MICB^{D136N} transductants to avoid expression bias (Figure 6A). Notably, Ba/F3.MICB^{D136N} had lower surface expression of MICB relative to Ba/F3.MICB^{WT} (Figures 6B and 6C).

We hypothesized that reduced surface MICB on MICB^{D136N} transductants may occur from differing antibody affinities for MICB or from destabilization of the protein. To assess surface expression of MICB independent of antibody affinity, we cultured Ba/F3 cells with His-tagged soluble recombinant NKG2D protein (sNKG2D). Indeed, more sNKG2D was detected on Ba/F3.MICB^{WT} than Ba/F3.MICB^{D136N} (Figures 6D and 6E). These findings suggest that there was less surface MICB on Ba/F3.MICB^{D136N} cells and that D136N may result in decreased affinity for NKG2D.

We investigated the functional significance of MICB^{D136N}. We designed BWZ cells to report NKG2D receptor activity in an NFAT (nuclear factor of activated T cells)-dependent manner (Figure E4A) (32). We confirmed that the chimeric receptor on BWZ.ζ-NKG2D was functional by stimulating cells using plate-bound anti-human NKG2D antibody. Cocultures of

Table 2. Vanderbilt Validating Acute Lung Injury Biomarkers for Diagnosis and Acute Respiratory Distress Syndrome Cohort Baseline Characteristics

Variable	Sepsis Cohort (*N* = 1,376)	ARDS Cohort (*N* = 733)
Sex, male	780 (56.7)	437 (60)
Ethnicity		
White	1,184 (86)	636 (87)
Non-White	192 (14)	97 (13)
rs1051788		
GG & GA	1,211 (88)	651 (88.8)
AA	165 (12)	82 (11.2)
Age, yr	55.2 (45–66)	53 (39–63)
Lowest P:F ratio, mm Hg	152 (102–217)	114 (79–158)
APACHE II score	27 ± 8.2	28 ± 7.7

Definition of abbreviations: APACHE = Acute Physiology and Chronic Health Evaluation; P:F = Pa_{O_2} to FI_{O_2}.
Data are presented as *n* (%), median (interquartile range), or mean ± SD.

BWZ.ζ-NKG2D reporter cells and Ba/F3 cells expressing MICB proteins revealed two patterns. With lower stimulation, $MICB^{WT}$ induced greater NKG2D receptor activation relative to Ba/F3 $MICB^{D136N}$ cells (Figure 7A), but, at higher stimulation, NKG2D activation plateaued for Ba/F3.$MICB^{WT}$ cells and was less than the Ba/F3 $MICB^{D136N}$ stimulus (Figure 7B).

To determine if these results were due to downregulation of the NKG2D receptor from efficient engagement, we performed cocultures of BWZ.ζ-NKG2D cells with Ba/F3 transductants and assessed NKG2D surface expression. Indeed, Ba/F3.$MICB^{WT}$ cell stimulation caused more substantial downregulation of surface NKG2D than the Ba/F3 $MICB^{D136N}$ cells (Figures E4B and 7C). This suggested that $MICB^{WT}$ protein has a higher affinity for NKG2D than $MICB^{D136N}$ and drives receptor endocytosis upon engagement. Collectively, these results show that D136N destabilizes MICB expression at the surface of cells and results in lower engagement of NKG2D at physiologic amounts.

We repeated all experiments in a different cell line to confirm that findings were independent of target cell type. We transfected HEK293T, an immortalized cell line derived from human embryonic kidney cells, using the same MICB vectors (Figure E5A). We gated for EGFP (Figure E5B) and noted a similar reduction in MICB surface expression among HEK293T.$MICB^{D136N}$ transfectants (Figure E5C). In addition, we determined that HEK293T.$MICB^{D136N}$ cells less often bound soluble NKG2D protein (Figures E5D and E5F). These findings suggest that the $MICB^{D136N}$ variant confers altered surface protein and decreased NKG2D signaling independent of cell type.

NKG2D-mediated NK Cell Activation and NK-mediated Killing of Primary Airway Cells Is Reduced in the Context of the D136N Variant

To determine the functional significance of $MICB^{D136N}$, we used the human NK cell line NK92 as effectors in coculture assays. Upon engagement with a ligand, NKG2D undergoes ubiquitylation of DAP10 and receptor endocytosis, which increases NK cell functional responses (43). Thus, we measured NKG2D surface expression as a

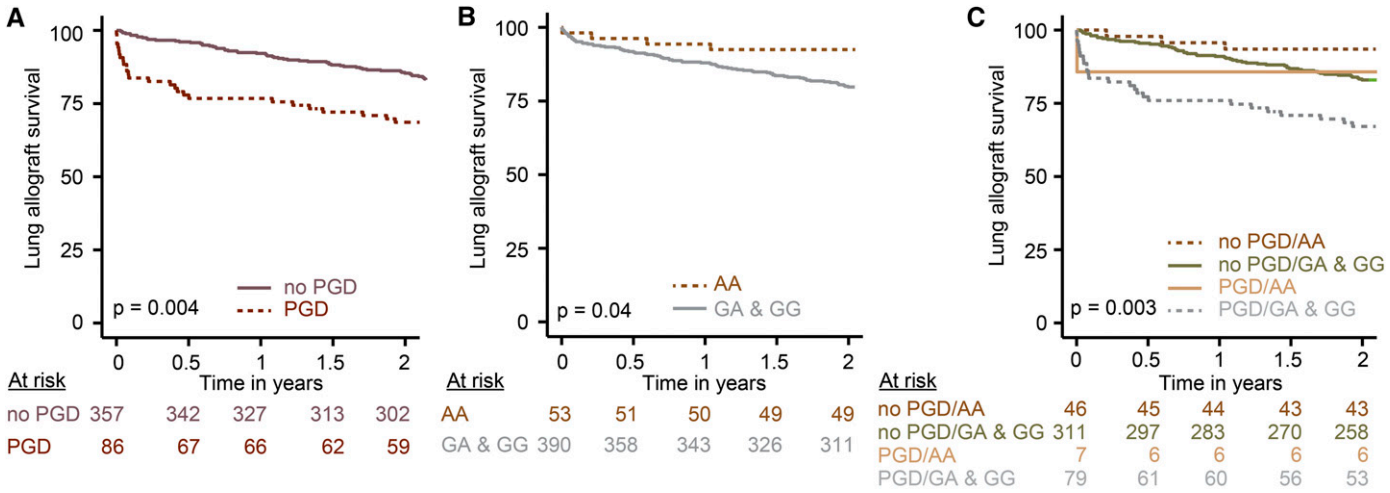

Figure 3. Reduced risk of allograft failure and death among donor $MICB^{G406A}$ genotypes. Kaplan-Meier plots show freedom from retransplantation and death within the LTOG (Lung Transplant Outcomes Group) cohort for the 443 participants with complete longitudinal follow-up data available. (*A*) The 86 subjects with severe primary graft dysfunction (PGD) had increased risk for lung allograft failure (hazard ratio [HR], 1.6; 95% confidence interval [CI], 1.2–2.2; $P = 0.004$) relative to 357 subjects without PGD. (*B*) There was one-third of the risk of allograft failure or death among participants homozygous for donor $MICB^{G406A}$ (HR, 0.36; 95% CI, 0.13–0.98; adjusted $P = 0.04$) relative to other genotypes. (*C*) We stratified participants with PGD by *MICB* rs1051788 genotype and found no difference in risk of allograft failure among $MICB^{G406A}$-homozygous donors irrespective of PGD status, but a sixfold increased risk of retransplantation and death among carriers of $MICB^{WT}$ alleles with severe PGD ($n = 79$; 95% CI, 1.8–20.1; adjusted $P = 0.003$) compared with $MICB^{G406A}$-homozygous donors without PGD. Risk for retransplantation or death was assessed by Cox proportional hazards models adjusted for participant baseline characteristics.

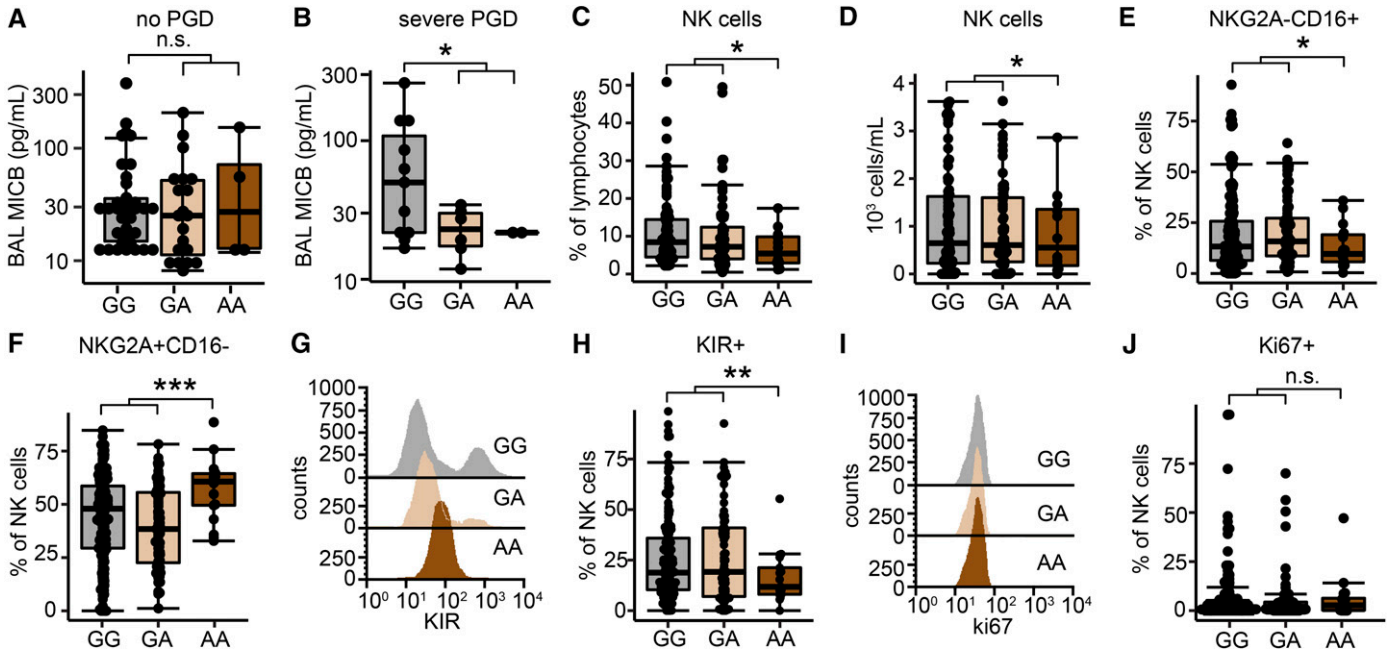

Figure 4. Donor *MICB*^{G406A} genotypes are associated with reduced quantities and more immature bronchoalveolar lavage natural killer (NK) cells. We prospectively collected BAL fluid from 77 lung transplant recipients and separately followed 102 recipients for BAL NK cell immunophenotyping at a single center. (*A*) BAL MICB protein in recipients without primary graft dysfunction (PGD) by donor MICB genotype. (*B*) BAL MICB protein in recipients with severe PGD by donor MICB genotype. (*C*) NK cells ($CD3^{-}CD56^{+}$) were decreased among recipients with *MICB*^{G406A} genotypes both as a percentage of lymphocytes and (*D*) in absolute NK cells/ml of BAL fluid compared with carriers of *MICB*^{WT} alleles. NK cell maturation was assessed by loss of NKG2A and gain of CD16. (*E*) We identified reduced frequencies of mature $NKG2A^{-}CD16^{+}$ NK cells among participants homozygous for donor *MICB*^{G406A} and (*F*) increased frequencies of BAL immature NK cells ($NKG2A^{+}CD16^{-}$) among participants homozygous for the *MICB*^{G406A} allele. (*G* and *H*) Representative histograms of NK cell KIR (Killer cell Immunoglobulin-like Receptor) staining show that participants with *MICB*^{G406A} had BAL NK cells with lower frequencies of surface KIR, as quantified in *H*. (*I* and *J*) We measured cell proliferation by Ki67 staining and found no differences across genotypes. Immunophenotype comparisons were assessed with generalized estimating equation–adjusted linear models to account for repeat measures, with significance levels noted as $^{*}P < 0.05$, $^{**}P < 0.01$, and $^{***}P < 0.001$. n.s. = not significant.

surrogate for NK cell activation. We found reduced NKG2D receptor endocytosis on NK92 cells in cultures with MICB^{D136N} transductants and higher NKG2D endocytosis in cultures with Ba/F3 MICB^{WT} transductants relative to control groups (Figures 7D and 7E). NK92 killing of Ba/F3 cell lines (Figures E6A and E6B) and NK cell IFNγ release did not differ between wild-type and MICB^{D136N} transductants (Figure E6C).

To assess how MICB^{D136N} influences airway cytotoxicity, we obtained primary human tracheal epithelial cells from a donor with MICB^{WT} and a donor with MICB^{D136N} and cocultured the epithelial cells with primary human NK cells (Figure 7F). Samples were matched for CMV serology, HLA-Bw6, donor age, and sample age, although this captures only some of the complexity of NK cell receptor–ligand interactions. We found reduced NK cell killing of hypoxic MICB^{D136N} epithelial cells relative to hypoxic MICB^{WT} epithelial cells (Figure 7G). We also measured induction of surface MICB on these cells in response to hypoxia (Figure 7H). Notably, MICB^{D136N} airway cells had less induction of MICB protein by median fluorescent intensity (Figure 7I) and as a percentage of total epithelial cells (Figure 7J) relative to MICB^{WT} airway cells. These results suggest that MICB^{D136N} results in reduced NK cell function and cytotoxicity as well as blunted surface MICB induction in response to hypoxia.

Discussion

Within two large cohorts, we found that a common SNP in a NKG2D receptor ligand gene, *MICB*, was associated with reduced incidence of severe ALI. We identified that the variant protein MICB^{D136N} results in lower surface MICB, reduced NKG2D signaling, and reduced NK cell function. Together, these findings reveal a novel mechanism of ALI (Figure 8).

We previously demonstrated that MICB protein and NK cell transcripts are increased in the BAL of recipients with severe PGD (20). In mouse experimental models of PGD, we found that injury occurred in an NK cell NKG2D receptor–dependent manner (20). In the current study, we show that genotypes encoding MICB^{D136N} confer reduced NK cell activation and are associated with less ALI and better survival. These findings bridge results of the mouse studies with observational human data. They represent a natural trial of dampening the receptor–ligand interaction between NKG2D and MICB and support direct targeting of this mechanism in clinical interventions (44).

The finding that MICB^{D136N} confers improved outcomes across PGD and ARDS further cements shared pathophysiology between these two syndromes. NK cell

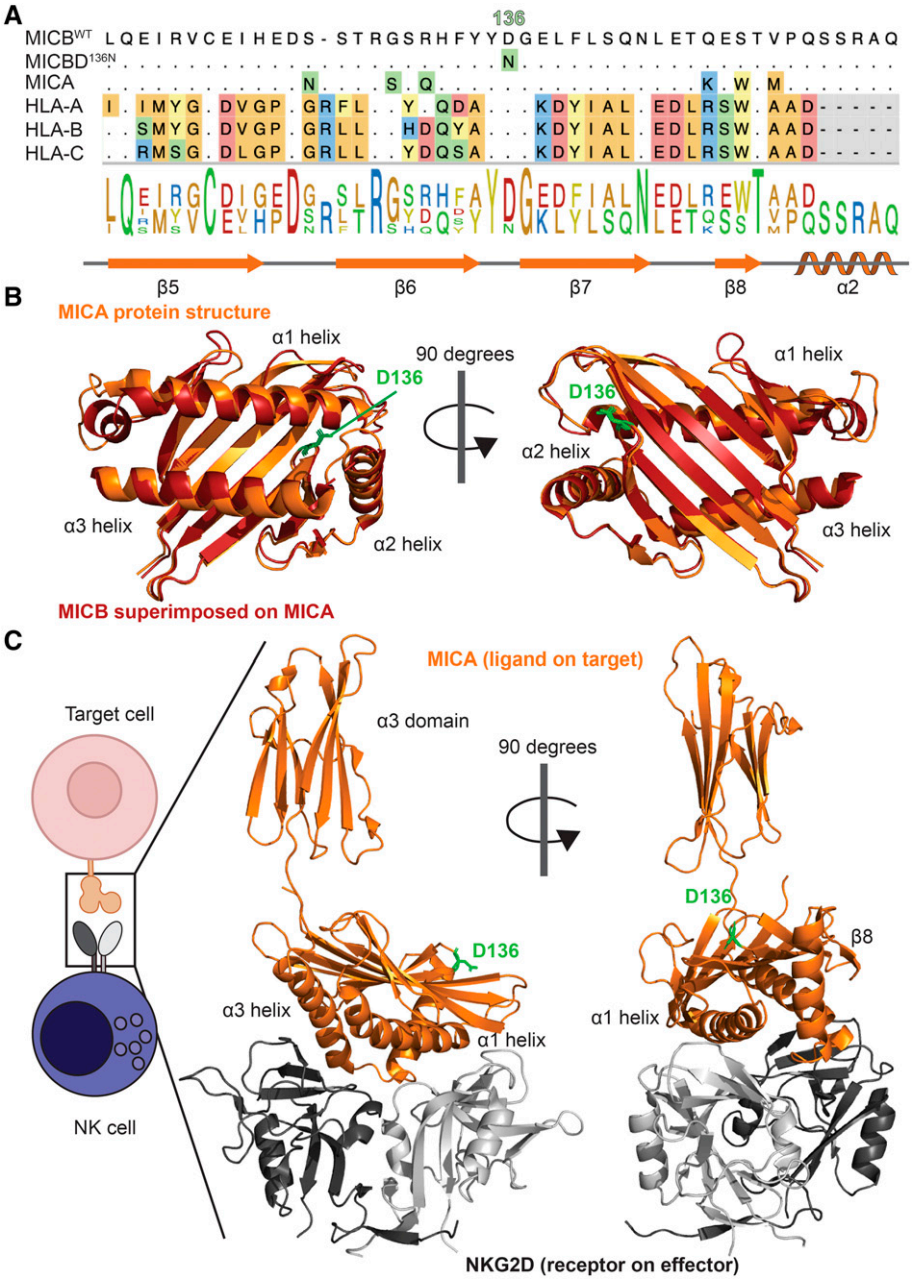

Figure 5. *MICB*^{G406A} genomic variant encodes a D136N amino acid substitution and protein structural perturbation. (*A*) Amino acid sequences of MICB^{WT}, MICB^{D136N}, MICA, HLA-A, HLA-B, and HLA-C were aligned using ClustalW and demonstrated conservation of aspartic acid at position 136 on MICB. The graphic below the sequence shows the position of the β strands and α helices. (*B*) Structural overlays of the α1 and α2 domains of MICB (red, PDB: 2WY3) and MICA (orange, PDB: 2WY3). Green residue demonstrates Asp/Asn at position 136. (*C*) Cocrystal structure of MICA complexed with NKG2D highlighting position of the Asp at position 136 relative to interaction surface. MICA is shown in orange, whereas dimer of NKG2D is shown as hues of gray. NK = natural killer.

signatures have been described in ARDS, but further work is required to establish the role of NKG2D-ligand mechanisms in ARDS samples (45, 46). Lungs experience frequent inflammatory insults compared with other organs (47–50). This stress evokes phenotypes from polymorphisms within innate immune cells that would not otherwise be evident. Notably, SNPs in the fungal recognition receptor gene *CLEC7A* and the innate sensor gene *TLR4* have been associated with chronic rejection and death in lung allograft recipients (22, 51). Downstream of *TLR4*, a polymorphism in *PTX3* (pentraxin-3) has been associated with increased risk for PGD (27). Our findings extend this observation and shed light on a novel receptor–ligand interaction.

Our data also suggest that the *MICB* gene may impact NK cell education. Donor *MICB*^{WT} allografts had more mature BAL

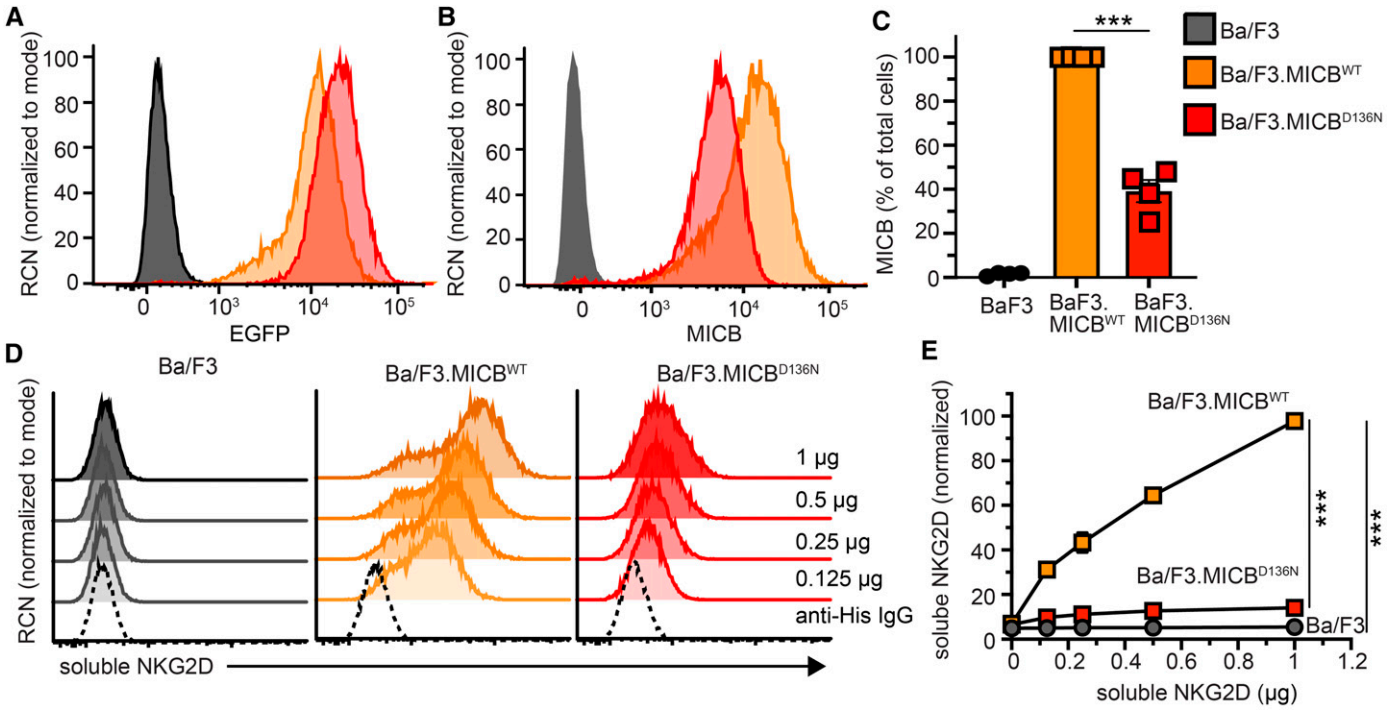

Figure 6. Reduced surface MICB and NKG2D binding on cells with the D136N substitution. (*A*) Ba/F3 cells expressing MICB^{WT} (orange) and MICB^{D136N} (red) mutation were generated and sorted for cell surface expression of EGFP (enhanced green fluorescent protein). (*B*) After sorting for EGFP, MICB was assessed on the cell surface with anti-MICB antibody staining using flow cytometry. (*C*) Surface MICB expressed as a normalized mean fluorescence intensity normalized to MICB^{WT}. Data summary of four independent experiments. (*D*) Ba/F3 cells were stained with soluble recombinant His-tagged NKG2D protein and then stained for anti-His antibody to detect presence of NKG2D on the cell surface using flow cytometry. (*E*) Quantitation of data in *D*. Data representative of two independent experiments performed in duplicate and graphs show mean ± SD. ***$P < 0.001$ as determined by one-way ANOVA with Tukey *post hoc* test. RCN = relative channel number.

NK cells than *MICB*^{G406A}-homozygous allografts. We suspect that these NK cells follow a shed NKG2D ligand concentration gradient (52–55). Potential stressors that evoke NKG2D ligands during thoracic transplant include hypoxia, donor tobacco exposure, and recipient pulmonary hypertension. The question remains of which cells are injured and flagging stress during PGD. Our mouse models suggest the dominant cell types are epithelial cells, which is supported by publicly available human lung atlas data (Figure EF7). Although we did not directly measure NKG2D in BAL NK cells, there is evidence that mature NK cells have less surface NKG2D than immature NK cells (56). The findings shown here suggest that the interaction between recipient NK cells and the donor *MICB* genotype may influence NK cell phenotypes. Additional study is required to understand if *MICB*^{G406A} alters the response to other NK cell–associated pulmonary syndromes, such as CMV or antibody-mediated injury. These results provide a molecular basis for previously described associations between MICB^{G406A} and herpes simplex virus infection (21).

Our *in vitro* data reveal clear differences in MICB expression, NKG2D receptor stimulation, NKG2D receptor endocytosis, and NKG2D-dependent NK cell killing between MICB^{D136N} and MICB^{WT} protein variants. However, the relevance of these molecular findings to the human clinical data is incompletely determined. *MICB*^{D136N} may alter protein trafficking or degradation leading to reduced surface protein expression. Based on our protein modeling, Asp136 is not in the NKG2D receptor–binding domain, but MICB^{D136N} may indirectly impact the stability of the MICB:NKG2D interaction through global protein conformational changes. It is unlikely for Asp136 to act as a substrate for glycosylation, as the optimal sequence would be N-X-S/T, with X being any amino acid except proline, followed by serine or threonine. This is not the case at position 136 (57). Further biochemical studies may address these questions through affinity and cocrystal analyses.

This study has some limitations. The genotype analyses were conducted across two North American cohorts in which we observed a high minor allele frequency. Notably, populations enriched for individuals of African, East Asian, and Hispanic ancestries (Figure E2), may have differing allele frequencies. Thus, incorporating rs1051788 into genomic screens should be considered in the context of the population's ancestral admixture. In addition, the LTOG cohort does not have data on chronic lung allograft dysfunction gradings, an important lung transplant outcome that would inform clinical trials targeting this mechanism. Our secondary analyses of ventilator-free days and mortality in the VALID cohort revealed trends for improved outcomes in the MICB-variant patients, consistent with expectations based on the absolute P:F ratio differences. However, our cohort lacked power to detect small differences in mortality. We found no differences in NK cell killing of Ba/F3 transductants, which may be due to alternate receptor activation, the relatively high basal

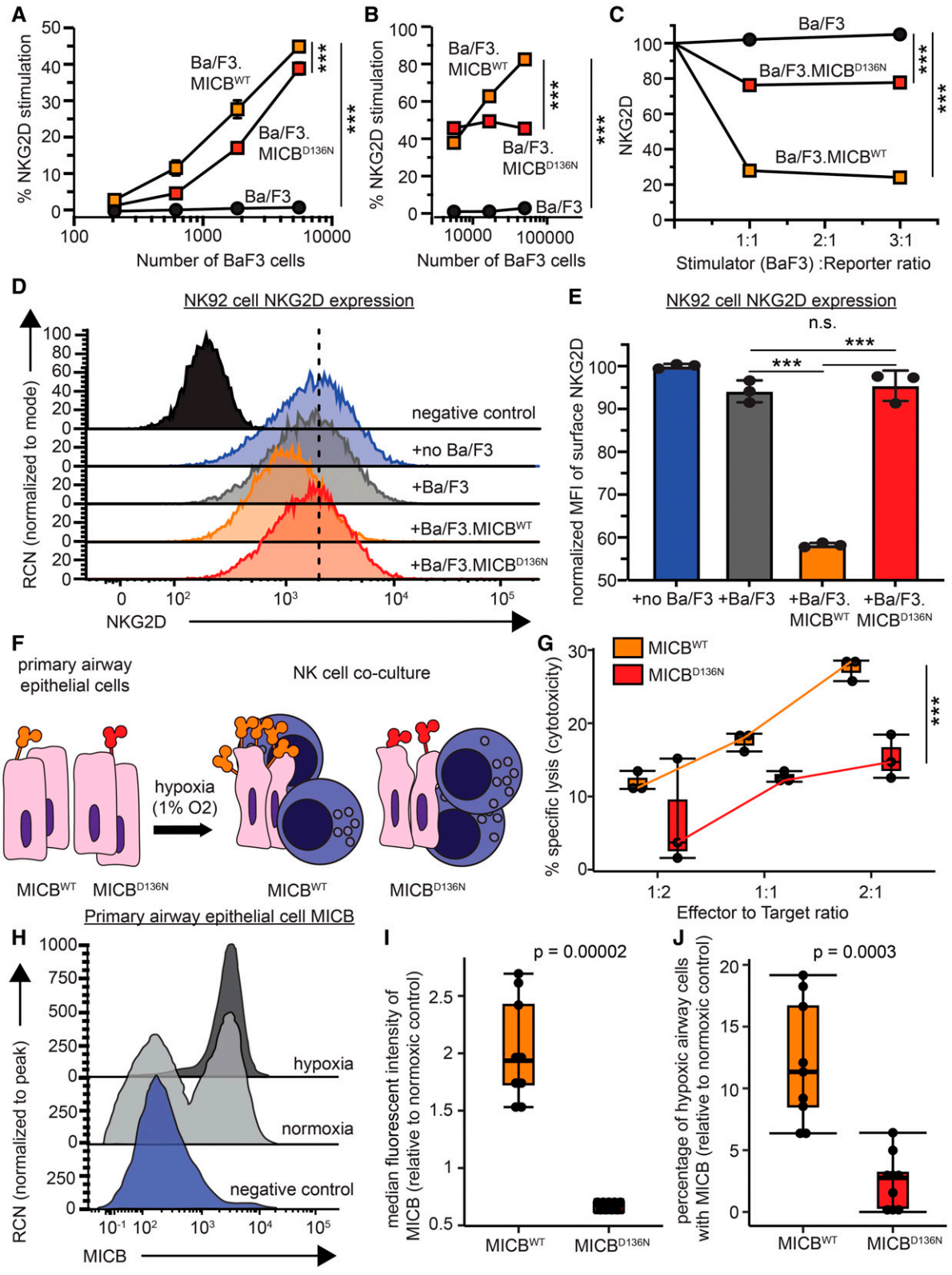

Figure 7. D136N substitution alters NKG2D receptor signaling. BWZ.ζ-NKG2D reporter cells were stimulated with MICB-transduced Ba/F3 cells to quantify NKG2D-specific signal transduction induced by MICB variants at (*A*) physiologic and (*B*) supraphysiologic stimulation. (*C*) Surface NKG2D on BWZ.ζ-NKG2D reporter cells after stimulation with Ba/F3 MICB variants. (*D*) NK92 cells were cocultured with parental Ba/F3 cells (gray), Ba/F3 expressing MICB^{WT} (orange) or MICB^{D136N} (red), or in the absence of Ba/F3 (blue) for 4 hours and then analyzed for surface

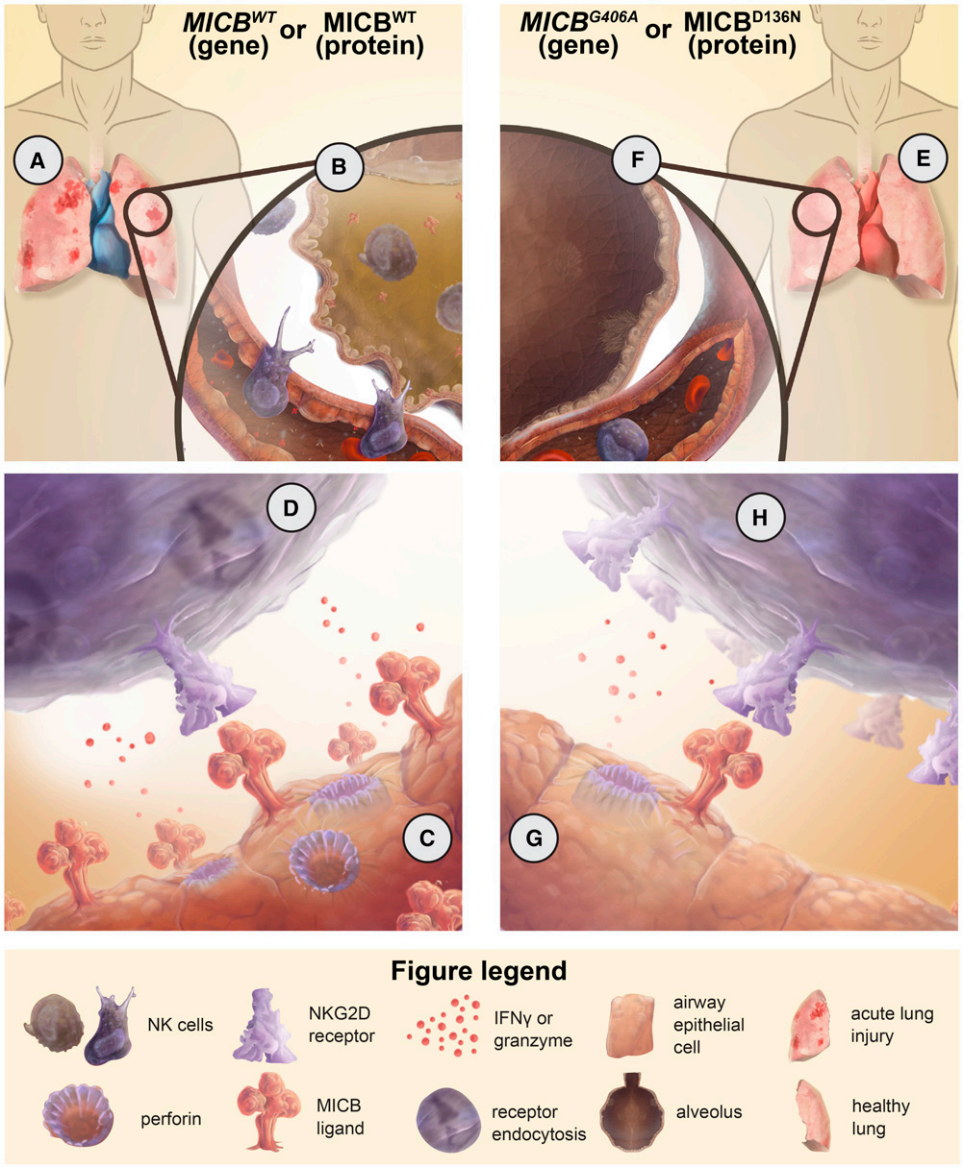

Figure 8. Schematic diagram of MICB in acute lung injury. Left two panels show findings in $MICB^{WT}$ participants and cells. Among $MICB^{WT}$ participants we found: (*A*) increased clinical acute lung injury (ALI), and (*B*) increased BAL natural killer (NK) cells and MICB stress molecules. (*C*) In MICB wild-type cell culture experiments, we found increased MICB on the surface of target cells and increased NK cell–mediated death. (*D*) NK cell NKG2D receptor was decreased. Right two panels show findings in $MICB^{G406A}$ participants and cells. We reported (*E*) less ALI and (*F*) fewer BAL NK cells and less MICB protein. In cell cultures, we reported (*G*) reduced surface MICB on target cells and less NK cell–mediated death, as well as (*H*) increased NK cell surface NKG2D.

Figure 7. (*Continued*). NKG2D expression using flow cytometry. (*E*) Quantitation of normalized data from *A*. (*F*) Schematic showing primary human airway epithelial cells from donors with $MICB^{WT}$ or $MICB^{D136N}$ cocultured with primary human natural killer (NK) cells. (*G*) Airway cell cytotoxicity relative to normoxic control cells across three effector-to-target ratios. (*H*) Representative mean fluorescence intensity (MFI) of MICB on epithelial cell surface. (*I*) MICB MFI relative to normoxic control. (*J*) Percentage of MICB on airway epithelial cells. Data are representative of two or three independent experiments performed in triplicate. Plots *A*–*E* show mean ± SD. Plots *G*, *I*, and *J* show medians, with bars representing 25th and 75th percentiles. *P* values are shown or represented by ***, which indicates statistical significance with $P < 0.001$. Differences were determined by one-way ANOVA with Tukey *post hoc* test (*A*–*E*) and Student's *t* test (*G*, *I*, and *J*). n.s. = not significant; RCN = relative channel number.

expression of MICB across both transductants, or differences in the threshold required for activation between NK cells educated *in vivo* and those cultured in IL-2. Finally, epithelial cell donors were matched, but killing by autologous NK cells may be subject to differential unmeasured receptor–ligand interactions. This study also has some notable strengths. The findings were validated across two large and broad patient cohorts focused on different ALI syndromes. We identified important clinical associations of the MICB variant and used multimodal approaches to show the molecular mechanism underlying a genomic determinant of lung injury and respiratory failure. The results confirm mechanistic findings from our prior animal models of the human syndrome.

In conclusion, we describe a novel mechanism of ALI pathogenesis with broad import to other organ injury syndromes. These findings identify the NKG2D receptor and ligand interaction as a promising therapeutic target (44, 58). ■

Author disclosures are available with the text of this article at www.atsjournals.org.

Acknowledgment: The authors thank the Lanier and Calabrese lab members for critical discussion of this work; the UCSF clinical team and fellow physicians for their instrumental aid in the collection of patient samples; Dr. Andrei Goga for use of the Tecan spectrophotometer; the UCSF Parnassus Flow Core (RRID:SCR_018206), which is supported by DRC Center grant NIH P30 DK063720, in part by grant NIH P30 DK063720, and by the NIH Instrumentation grant S10 1S10OD021822-01, for help and advice; and Nick Bezio for design of the schematic figure. They also thank the lung transplant donors and recipients for their generous gifts of life and knowledge.

References

1. Ware LB, Matthay MA. The acute respiratory distress syndrome. *N Engl J Med* 2000;342:1334–1349.
2. Bellani G, Laffey JG, Pham T, Fan E, Brochard L, Esteban A, *et al.*; LUNG SAFE Investigators; ESICM Trials Group. Epidemiology, patterns of care, and mortality for patients with acute respiratory distress syndrome in intensive care units in 50 countries. *JAMA* 2016;315:788–800.
3. Chambers DC, Perch M, Zuckermann A, Cherikh WS, Harhay MO, Hayes D Jr, *et al.*; International Society for Heart and Lung Transplantation. The International Thoracic Organ Transplant Registry of the International Society for Heart and Lung Transplantation. Thirty-eighth adult lung transplantation report – 2021: focus on recipient characteristics. *J Heart Lung Transplant* 2021;40:1060–1072.
4. Graham CN, Watson C, Barlev A, Stevenson M, Dharnidharka VR. Mean lifetime survival estimates following solid organ transplantation in the US and UK. *J Med Econ* 2022;25:230–237.
5. Whitson BA, Prekker ME, Herrington CS, Whelan TP, Radosevich DM, Hertz MI, *et al.* Primary graft dysfunction and long-term pulmonary function after lung transplantation. *J Heart Lung Transplant* 2007;26: 1004–1011.
6. Daoud D, Chacon Alberty L, Wei Q, Hochman Mendez C, Virk MHM, Mase J, *et al.* Incidence of primary graft dysfunction is higher according to the new ISHLT 2016 guidelines and correlates with clinical and molecular risk factors. *J Thorac Dis* 2021;13:3426–3442.
7. Diamond JM, Lee JC, Kawut SM, Shah RJ, Localio AR, Bellamy SL, *et al.*; Lung Transplant Outcomes Group. Clinical risk factors for primary graft dysfunction after lung transplantation. *Am J Respir Crit Care Med* 2013; 187:527–534.
8. Hamilton BC, Kukreja J, Ware LB, Matthay MA. Protein biomarkers associated with primary graft dysfunction following lung transplantation. *Am J Physiol Lung Cell Mol Physiol* 2017;312:L531–L541.
9. Morrison MI, Pither TL, Fisher AJ. Pathophysiology and classification of primary graft dysfunction after lung transplantation. *J Thorac Dis* 2017;9: 4084–4097.
10. Calabrese DR, Aminian E, Mallavia B, Liu F, Cleary SJ, Aguilar OA, *et al.* Natural killer cells activated through NKG2D mediate lung ischemia-reperfusion injury. *J Clin Invest* 2021;131:e137047.
11. Calabrese DR, Lanier LL, Greenland JR. Natural killer cells in lung transplantation. *Thorax* 2019;74:397–404.
12. Lanier LL. NK cell recognition. *Annu Rev Immunol* 2005;23:225–274.
13. Bauer S, Groh V, Wu J, Steinle A, Phillips JH, Lanier LL, *et al.* Activation of NK cells and T cells by NKG2D, a receptor for stress-inducible MICA. *Science* 1999;285:727–729.
14. Steinle A, Li P, Morris DL, Groh V, Lanier LL, Strong RK, *et al.* Interactions of human NKG2D with its ligands MICA, MICB, and homologs of the mouse RAE-1 protein family. *Immunogenetics* 2001; 53:279–287.
15. Lanier LL. NKG2D receptor and its ligands in host defense. *Cancer Immunol Res* 2015;3:575–582.
16. Klussmeier A, Massalski C, Putke K, Schäfer G, Sauter J, Schefzyk D, *et al.* High-throughput *MICA/B* genotyping of over two million samples: workflow and allele frequencies. *Front Immunol* 2020;11:314.
17. Feng L, Cheng F, Ye Z, Li S, He Y, Yao X, *et al.* The effect of renal ischemia-reperfusion injury on expression of RAE-1 and H60 in mice kidney. *Transplant Proc* 2006;38:2195–2198.
18. Luo L, Lu J, Wei L, Long D, Guo JY, Shan J, *et al.* The role of HIF-1 in up-regulating MICA expression on human renal proximal tubular epithelial cells during hypoxia/reoxygenation. *BMC Cell Biol* 2010;11:91.
19. Zhang Z-X, Wang S, Huang X, Min W-P, Sun H, Liu W, *et al.* NK cells induce apoptosis in tubular epithelial cells and contribute to renal ischemia-reperfusion injury. *J Immunol* 2008;181:7489–7498.
20. Calabrese DR, Tsao T, Magnen M, Valet C, Gao Y, Mallavia B, *et al.* NKG2D receptor activation drives primary graft dysfunction severity and poor lung transplantation outcomes. *JCI Insight* 2022;7:e164603.
21. Shirts BH, Kim JJ, Reich S, Dickerson FB, Yolken RH, Devlin B, *et al.* Polymorphisms in MICB are associated with human herpes virus seropositivity and schizophrenia risk. *Schizophr Res* 2007;94: 342–353.
22. Calabrese DR, Wang P, Chong T, Hoover J, Singer JP, Torgerson D, *et al.*; LTOG Investigators. Dectin-1 genetic deficiency predicts chronic lung allograft dysfunction and death. *JCI Insight* 2019;4:e133083.
23. Kerchberger VE, Bastarache JA, Shaver CM, Nagata H, McNeil JB, Landstreet SR, *et al.* Haptoglobin-2 variant increases susceptibility to acute respiratory distress syndrome during sepsis. *JCI Insight* 2019;4: e131206.
24. Calabrese DR, Chong T, Wang A, Singer JP, Gottschall M, Hays SR, *et al.* NKG2C natural killer cells in bronchoalveolar lavage are associated with cytomegalovirus viremia and poor outcomes in lung allograft recipients. *Transplantation* 2019;103:493–501.
25. Mallavia B, Liu F, Lefrançais E, Cleary SJ, Kwaan N, Tian JJ, *et al.* Mitochondrial DNA stimulates TLR9-dependent neutrophil extracellular trap formation in primary graft dysfunction. *Am J Respir Cell Mol Biol* 2020;62:364–372.
26. Prasad KM, Bamne MN, Shirts BH, Goradia D, Mannali V, Pancholi KM, *et al.* Grey matter changes associated with host genetic variation and exposure to Herpes Simplex Virus 1 (HSV1) in first episode schizophrenia. *Schizophr Res* 2010;118:232–239.
27. Diamond JM, Meyer NJ, Feng R, Rushefski M, Lederer DJ, Kawut SM, *et al.*; Lung Transplant Outcomes Group. Variation in PTX3 is associated with primary graft dysfunction after lung transplantation. *Am J Respir Crit Care Med* 2012;186:546–552.
28. Snell GI, Yusen RD, Weill D, Strueber M, Garrity E, Reed A, *et al.* Report of the ISHLT Working Group on Primary Lung Graft Dysfunction, part I: definition and grading. A 2016 Consensus Group statement of the International Society for Heart and Lung Transplantation. *J Heart Lung Transplant* 2017;36:1097–1103.
29. Ranieri VM, Rubenfeld GD, Thompson BT, Ferguson ND, Caldwell E, Fan E, *et al.*; ARDS Definition Task Force. Acute respiratory distress syndrome: the Berlin Definition. *JAMA* 2012;307:2526–2533.

30. Mesci A, Carlyle JR. A rapid and efficient method for the generation and screening of monoclonal antibodies specific for cell surface antigens. *J Immunol Methods* 2007;323:78–87.
31. Palacios R, Steinmetz M. Il-3-dependent mouse clones that express B-220 surface antigen, contain Ig genes in germ-line configuration, and generate B lymphocytes in vivo. *Cell* 1985;41:727–734.
32. Sanderson S, Shastri N. LacZ inducible, antigen/MHC-specific T cell hybrids. *Int Immunol* 1994;6:369–376.
33. Aguilar OA, Fong L-K, Ishiyama K, DeGrado WF, Lanier LL. The CD3ζ adaptor structure determines functional differences between human and mouse CD16 Fc receptor signaling. *J Exp Med* 2022;219: e20220022.
34. Balaji GR, Aguilar OA, Tanaka M, Shingu-Vazquez MA, Fu Z, Gully BS, *et al.* Recognition of host Clr-b by the inhibitory NKR-P1B receptor provides a basis for missing-self recognition. *Nat Commun* 2018;9: 4623.
35. Calabrese DR, Singer JP, Hays SR, Leard LE, Golden JA, Kolaitis NA, *et al.* Bronchoalveolar lavage MICB is associated with severe primary graft dysfunction, prolonged mechanical ventilation, and low post-transplant FEV_1 in lung transplant recipients. *J Heart Lung Transplant* 2022;41:S76.
36. O'Leary NA, Wright MW, Brister JR, Ciufo S, Haddad D, McVeigh R, *et al.* Reference sequence (RefSeq) database at NCBI: current status, taxonomic expansion, and functional annotation. *Nucleic Acids Res* 2016;44:D733–D745.
37. Knaus WA, Draper EA, Wagner DP, Zimmerman JE. APACHE II: a severity of disease classification system. *Crit Care Med* 1985;13: 818–829.
38. Valapour M, Lehr CJ, Schladt DP, Smith JM, Goff R, Mupfudze TG, *et al.* OPTN/SRTR 2021 annual data report: lung. *Am J Transplant* 2023;23: S379–S442.
39. Singer M, Deutschman CS, Seymour CW, Shankar-Hari M, Annane D, Bauer M, *et al.* The Third International Consensus Definitions for Sepsis and Septic Shock (Sepsis-3). *JAMA* 2016;315:801–810.
40. Ong DS, Klein Klouwenberg PM, Verduyn Lunel FM, Spitoni C, Frencken JF, Dekker HA, *et al.* Cytomegalovirus seroprevalence as a risk factor for poor outcome in acute respiratory distress syndrome. *Crit Care Med* 2015;43:394–400.
41. Müller S, Zocher G, Steinle A, Stehle T. Structure of the HCMV UL16-MICB complex elucidates select binding of a viral immunoevasin to diverse NKG2D ligands. *PloS Pathog* 2010;6:e1000723.
42. Li P, Morris DL, Willcox BE, Steinle A, Spies T, Strong RK. Complex structure of the activating immunoreceptor NKG2D and its MHC class I-like ligand MICA. *Nat Immunol* 2001;2:443–451.
43. Quatrini L, Molfetta R, Zitti B, Peruzzi G, Fionda C, Capuano C, *et al.* Ubiquitin-dependent endocytosis of NKG2D-DAP10 receptor complexes activates signaling and functions in human NK cells. *Sci Signal* 2015;8:ra108.
44. Vadstrup K, Bendtsen F. Anti-NKG2D mAb: a new treatment for Crohn's disease? *Int J Mol Sci* 2017;18:1997.
45. Sarma A, Christenson SA, Byrne A, Mick E, Pisco AO, DeVoe C, *et al.*; COMET Consortium. Tracheal aspirate RNA sequencing identifies distinct immunological features of COVID-19 ARDS. *Nat Commun* 2021;12:5152.
46. Sarma A, Christenson SA, Zha BS, Pisco AO, Neyton LPA, Mick E, *et al.* Hyperinflammatory ARDS is characterized by interferon-stimulated gene expression, T-cell activation, and an altered metatranscriptome in tracheal aspirates [preprint]. *medRxiv*; 2022 [accessed 2023 Jan 5]. Available from: https://www.medrxiv.org/content/10.1101/2022.03.31.22272425v1.
47. Allyn PR, Duffy EL, Humphries RM, Injean P, Weigt SS, Saggar R, *et al.* Graft loss and CLAD-onset is hastened by viral pneumonia after lung transplantation. *Transplantation* 2016;100:2424–2431.
48. Angaswamy N, Saini D, Ramachandran S, Nath DS, Phelan D, Hachem R, *et al.* Development of antibodies to human leukocyte antigen precedes development of antibodies to major histocompatibility class I-related chain A and are significantly associated with development of chronic rejection after human lung transplantation. *Hum Immunol* 2010;71:560–565.
49. Avery RK, Silveira FP, Benedict K, Cleveland AA, Kauffman CA, Schuster MG, *et al.* Cytomegalovirus infections in lung and hematopoietic cell transplant recipients in the Organ Transplant Infection Prevention and Detection Study: a multi-year, multicenter prospective cohort study. *Transpl Infect Dis* 2018;20:e12877.
50. Burton CM, Iversen M, Carlsen J, Mortensen J, Andersen CB, Steinbrüchel D, *et al.* Acute cellular rejection is a risk factor for bronchiolitis obliterans syndrome independent of post-transplant baseline FEV_1. *J Heart Lung Transplant* 2009;28:888–893.
51. Palmer SM, Burch LH, Davis RD, Herczyk WF, Howell DN, Reinsmoen NL, *et al.* The role of innate immunity in acute allograft rejection after lung transplantation. *Am J Respir Crit Care Med* 2003; 168:628–632.
52. Markiewicz MA, Wise EL, Buchwald ZS, Pinto AK, Zafirova B, Polic B, *et al.* RAE1ε ligand expressed on pancreatic islets recruits NKG2D receptor-expressing cytotoxic T cells independent of T cell receptor recognition. *Immunity* 2012;36:132–141.
53. Kawakami T, Ito K, Matsuda Y, Noda M, Sakurada A, Hoshikawa Y, *et al.* Cytotoxicity of natural killer cells activated through NKG2D contributes to the development of bronchiolitis obliterans in a murine heterotopic tracheal transplant model. *Am J Transplant* 2017;17:2338–2349.
54. Farhadi N, Lambert L, Triulzi C, Openshaw PJ, Guerra N, Culley FJ. Natural killer cell NKG2D and granzyme B are critical for allergic pulmonary inflammation. *J Allergy Clin Immunol* 2014;133:827–835.e3.
55. Vadstrup K, Galsgaard ED, Jensen H, Lanier LL, Ryan JC, Chen SY, *et al.* NKG2D ligand expression in Crohn's disease and NKG2D-dependent stimulation of $CD8^+$ T cell migration. *Exp Mol Pathol* 2017; 103:56–70.
56. Hood SP, Foulds GA, Imrie H, Reeder S, McArdle SEB, Khan M, *et al.* Phenotype and function of activated natural killer cells from patients with prostate cancer: patient-dependent responses to priming and IL-2 activation. *Front Immunol* 2019;9:3169.
57. Tan NY, Bailey U-M, Jamaluddin MF, Mahmud SHB, Raman SC, Schulz BL. Sequence-based protein stabilization in the absence of glycosylation. *Nat Commun* 2014;5:3099.
58. Paul P, Picard C, Sampol E, Lyonnet L, Di Cristofaro J, Paul-Delvaux L, *et al.* Genetic and functional profiling of CD16-dependent natural killer activation identifies patients at higher risk of cardiac allograft vasculopathy. *Circulation* 2018;137:1049–1059.